

## APPLICATION OF A DIFFERENTIAL EVOLUTION ALGORITHM WITH STRATEGY ADAPTATION TO THE DESIGN OF MULTI-BAND MICROWAVE FILTERS FOR WIRELESS COMMUNICATIONS

**S. K. Goudos and Z. D. Zaharis**

Telecommunications Center  
Aristotle University of Thessaloniki, Thessaloniki 54124, Greece

**T. V. Yioultsis**

Department of Electrical and Computer Engineering  
Aristotle University of Thessaloniki, Thessaloniki 54124, Greece

**Abstract**—In this paper, we present a new method for the design of multi-band microstrip filters. The proposed design method is based on Differential Evolution (DE) with strategy adaptation. This self-adaptive DE (SaDE) uses previous experience in both trial vector generation strategies and control parameter tuning. We apply this algorithm to two design cases of dual and tri-band filters for WiFi and WiMax applications. We select the Open Loop Ring Resonator (OLRR) filters, which are comprised of two uniform microstrip lines and pairs of open loops between them. The results indicate the advantages of this approach and the applicability of this design method.

### 1. INTRODUCTION

Microwave filters are among the important components of a modern wireless communication system. Several papers exist in the literature that address the filter design problem [1–14]. Bandpass filter design is presented in [5, 7, 8, 10, 11] using different filter structures like hexagonal loop resonators, radial line stubs, parallel-coupled lines, spiral shaped resonators, and half mode substrate integrated folded waveguide. Microstrip ultra-wideband filter design is given in [2, 4], while in [1, 13, 14] dual-band filters are designed. Open Loop Ring

Resonator (OLRR) filters, which consist of two uniform microstrip lines and pairs of open loops between them, are widely used as the building block in several multiband bandpass filter design cases [15–17]. In [15], two pairs of folded OLRRs operating at two passbands are proposed to produce dual-band response. In [18], a tri-band bandpass filter is constructed by using three pairs of stub loaded OLRRs. In [19], the space-mapping technique is used for OLRR filter design. This is accomplished in conjunction with FEKO [20] a commercially available EM solver. FEKO is a hybrid MoM/FEM software, which we also use for the OLRR filter design.

Evolutionary algorithms (EAs) like Genetic Algorithms (GAs), Particle Swarm Optimization (PSO) and Differential Evolution (DE) have been applied to a variety of design problems in electromagnetics [21–38]. In [21], Multi-objective Particle Swarm Optimization with fitness sharing (MOPSO-fs) is applied to a multilayer dielectric filter design problem while in [32] multi-objective DE is used for both dielectric filter design and bandpass OLRR filter design. Differential evolution (DE) [39,40] is a population-based stochastic global optimization algorithm, which has been used in several real world engineering problems like fuzzy logic controller design problem [41], molecular sequence alignment problem [42], and automatic image pixel clustering [43]. Several DE variants or strategies exist. One of the DE advantages is that very few control parameters have to be adjusted in each algorithm run. However, the control parameters involved in DE are highly dependent on the optimization problem. Moreover, the selection of the appropriate strategy for trial vector generation requires additional computational time using a trial-and-error search procedure. Therefore, it is not always an easy task to fine-tune the control parameters and strategy. A DE strategy that self-adapts the control parameters has been introduced in [44]. This algorithm has been applied successfully to a microwave absorber design problem [45] and linear array synthesis [33]. A DE algorithm that self-adapts both control parameters and strategy based on learning experiences from previous generations is presented in [46–48]. That way expensive computational costs spent on searching using a trial-and-error procedure can be avoided. The novelty in our work lies in the fact that we present a design framework for microwave filters based on SaDE. To the best of our knowledge, this is the first time that the SaDE algorithm is applied to a microwave filter design problem.

This paper is organized as follows: Section 2 describes the problem formulation and objective function. A brief description of the SaDE algorithm is given in Section 3. Section 4 presents the numerical results for two distinct filter design cases. Finally, the conclusion is given in

Section 5.

**2. OPEN LOOP RING RESONATOR FILTERS**

A dual band OLRR filter is shown in Figure 1. The frequency response of such a filter depends on the filter dimensions and spacings between microstrip lines [15, 19]. The design parameters for this case are the ones shown in Figure 1, ( $W_1, W_2, L_1, L_2, L_3, L_4, L_5, S_1, S_2, S_3, G$ ), all expressed in mm. A corresponding tri-band filter can be realized using three pairs of open loops. The geometry of a tri-band filter is shown in Figure 2. The design parameters of the tri-band filter are ( $W_1, W_2, L_1, L_2, L_3, L_4, L_5, L_6, S_1, S_2, S_3, G_1, G_2$ ).

Such a filter design problem can be defined by the minimization of  $|S_{11}|$  in the passband frequency range. This design problem is therefore defined by the minimization of the objective function:

$$F(\bar{x}) = 20 \log \{ \max |S_{11}(\bar{x}, f)|, f \in S_p \} \tag{1}$$

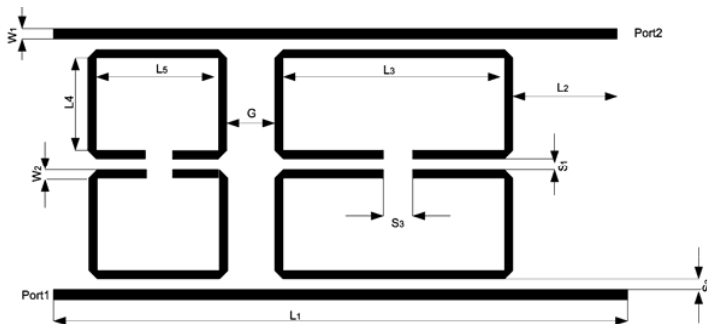


**Figure 1.** Dual-band filter geometry.

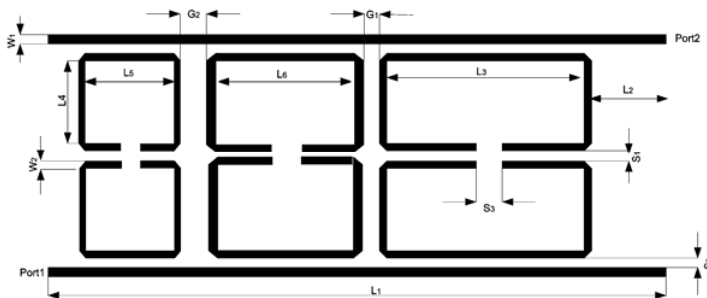


**Figure 2.** Tri-band filter geometry.

where  $\bar{x}$  is the vector of filter geometry parameters and  $S_p$  is the set of distinct frequencies in the desired passband frequency ranges.

### 3. THE DIFFERENTIAL EVOLUTION ALGORITHM

A population in DE consists of  $NP$  vectors  $\bar{x}_{G,i}$ ,  $i = 1, 2, \dots, NP$ , where  $G$  is the generation number. The population is initialized randomly from a uniform distribution. Each  $D$ -dimensional vector represents a possible solution. The initial population evolves in each generation with the use of three operators: mutation, crossover and selection. Depending on the form of these operators several DE variants or strategies exist in the literature [40, 49]. The choice of the best DE strategy depends on problem type [50]. In SaDE the following four strategies are used for trial vector generation. These include *DE/rand/1/bin*, *DE/rand-to-best/2/bin*, *DE/rand/2/bin*, and *DE/current-to-rand/1* [51]. In these strategies, a mutant vector  $\bar{v}_{G+1,i}$  for each target vector  $\bar{x}_{G,i}$  is computed by:

*DE/rand/1/bin*

$$\bar{v}_{G+1,i} = \bar{x}_{G,r_1} + F(\bar{x}_{G,r_2} - \bar{x}_{G,r_3}), \quad r_1 \neq r_2 \neq r_3$$

*DE/rand-to-best/2/bin*

$$\bar{v}_{G+1,i} = \bar{x}_{G,i} + F(\bar{x}_{G,best} - \bar{x}_{G,i}) + F(\bar{x}_{G,r_1} - \bar{x}_{G,r_2}) + F(\bar{x}_{G,r_3} - \bar{x}_{G,r_4}), \quad r_1 \neq r_2 \neq r_3 \neq r_4$$

*DE/rand/2/bin*

$$\bar{v}_{G+1,i} = \bar{x}_{G,r_1} + F(\bar{x}_{G,r_2} - \bar{x}_{G,r_3}) + F(\bar{x}_{G,r_4} - \bar{x}_{G,r_5}), \quad r_1 \neq r_2 \neq r_3 \neq r_4 \neq r_5$$

*DE/current-to-rand/1/bin*

$$\bar{v}_{G+1,i} = \bar{x}_{G,i} + K(\bar{x}_{G,r_1} - \bar{x}_{G,i}) + F(\bar{x}_{G,r_2} - \bar{x}_{G,r_3}), \quad r_1 \neq r_2 \neq r_3$$

where  $r_1, r_2, r_3, r_4, r_5$  are randomly chosen indices from the population, which are different from index  $i$ ,  $F$  is a mutation control parameter,  $K$  a coefficient responsible for the level of recombination that occurs between  $\bar{x}_{G,i}$  and  $\bar{x}_{G,r_1}$ . After mutation, the crossover operator is applied to generate a trial vector  $\bar{u}_{G+1,i} = (u_{G+1,1i}, u_{G+1,2i}, \dots, u_{G+1,ji}, \dots, u_{G+1,Di})$  whose coordinates are given by:

$$u_{G+1,ji} = \begin{cases} v_{G+1,ji}, & \text{if } \text{rand}_{j[0,1]} \leq CR \text{ or } j = rn(i) \\ x_{G+1,ji}, & \text{if } \text{rand}_{j[0,1]} > CR \text{ and } j \neq rn(i) \end{cases} \quad (3)$$

where  $j = 1, 2, \dots, D$ ,  $\text{rand}_{j[0,1]}$  is a number from a uniform random distribution from the interval  $[0,1]$ ,  $rn(i)$  a randomly chosen index from  $(1, 2, \dots, D)$ , and  $CR$  the crossover constant from the interval  $[0, 1]$ .

DE uses a greedy selection operator, which for minimization problems is defined by:

$$\bar{x}_{G+1,i} = \begin{cases} \bar{u}_{G+1,i}, & \text{if } f(\bar{u}_{G+1,i}) < f(\bar{x}_{G,i}) \\ \bar{x}_{G,i}, & \text{otherwise} \end{cases} \quad (4)$$

where  $f(\bar{u}_{G+1,i})$ ,  $f(\bar{x}_{G,i})$  are the fitness values of the trial and the old vector respectively. Therefore, the newly found trial vector  $\bar{u}_{G+1,i}$  replaces the old vector  $\bar{x}_{G,i}$  only when it produces a lower objective-function value than the old one. Otherwise, the old vector remains in the next generation. The stopping criterion for the DE is usually the generation number or the number of objective-function evaluations.

### 3.1. DE with Strategy Adaptation (SaDE)

In the SaDE algorithm, both the trial vector generation strategies and the control parameters are self-adapted according to previous learning experiences. SaDE maintains a strategy candidate pool, consisting of the four strategies given in (2). Each strategy is assigned a certain probability. The sum of all probabilities is equal to one. These probabilities are initialized with a value of 0.25 and gradually adapted during evolution. The probability of applying the  $m$ -th strategy is  $p_m$ ,  $m = 1, 2, \dots, M$ , where  $M$  is the total number of strategies. At generation  $G$ , the number of successful trial vectors generated by the  $m$ -th strategy is denoted as  $ns_{m,G}$ , while the number of trial vectors that fail to replace the old vectors in the next generation is  $nf_{m,G}$ . An additional parameter called the learning period (LP) is introduced in [48]. This corresponds to the number of the previous generations that store the success and fail statistics. After LP generations, the probabilities of selecting different strategies are updated according to:

$$p_{m,G} = \frac{S_{m,G}}{\sum_{m=1}^M S_{m,G}} \quad (5)$$

$$\text{where, } S_{m,G} = \frac{\sum_{g=G-LP}^{G-1} ns_{m,g}}{\sum_{g=G-LP}^{G-1} ns_{m,g} + \sum_{g=G-LP}^{G-1} nf_{m,g}} + \varepsilon$$

where  $S_{m,G}$  is the success rate of the trial vectors generated by the  $m$ -th strategy within the previous LP generation and  $\varepsilon$  is a constant set equal to 0.01 to avoid possible null success rates. Therefore, according to (5) strategies with high success rates have higher probability to be applied at the current generation.

The control parameters are self-adapted in the following way. The mutation control parameter  $F$  is approximated by a normal distribution with mean value 0.5 and standard deviation 0.3, that is  $N(0.5, 0.3)$ . The parameter  $K$  is a random number in the interval  $[0, 1]$  generated by a uniform distribution. The crossover rate control parameter  $CR$  used by the  $m$ -th strategy is also approximated by a normal distribution with mean value  $CR_m$  and standard deviation 0.1, that is  $N(CR_m, 0.1)$ . The initial value of  $CR_m$  is 0.5 for all strategies. The values of crossover rates that have successfully generated trial vectors in the previous LP generations are stored in a crossover rate memory for each strategy  $CR_m^{memory}$  that is an array of size LP. At each generation, the median value stored in memory for the  $m$ -th strategy  $CR_m^{median}$  is calculated and the  $CR$  values generated are given by a normal distribution with mean value  $CR_m^{median}$  and standard deviation 0.1. That way the crossover values are evolved at each generation to follow the successful values found. More details about the SaDE algorithm can be found in [48].

#### 4. NUMERICAL RESULTS

The OLR filters are modeled in FEKO. Both filters are fabricated on a substrate with dielectric constant 9.79 and height 26.5 mils (0.6731 mm). An empirical rule in DE [39, 40] states that the population size should be set to  $10D$ , where  $D$  is the problem dimension. That would require a population size of 110 and 130 vectors for the dual-band and the tri-band case respectively. Such vector numbers would significantly increase the total computational cost. Using a trial and error search we have found that 20 vectors is an adequate population size for that design problems. The total number of generations is set to 500. The best results after 10 independent trials are selected. The  $LP$  value is set to 20. The authors in [48] suggest a value between 20 and 60 for the parameter LP. The sensitivity analysis performed in [48] for the LP parameter showed it had no significant impact on SaDE performance. All algorithm runs are performed on a PC with Intel Core 2 Duo E8500 at 3.16 GHz with 4 GB RAM.

In order to integrate the in-house source code of the SaDE algorithm with FEKO, a wrapper program was created. FEKO, except for using a graphical user interface, offers the option to run the EM solver engine from command line. It requires an input file that defines the model geometry. This input file uses a script language that allows users to define variables and control options like the frequency range, the number of frequency points and the required data in the output file. The wrapper creates a FEKO input file for each random vector

created by the algorithms and runs FEKO. The output file, which in our case is defined to contain the frequency and the  $S$ -parameters is read by the wrapper and the objective function is evaluated.

#### 4.1. Dual-band Filter Design Case

The first filter is designed for operation in two WiMax (IEEE 802.16) frequency bands. These are the 3.5 GHz and the 5.8 GHz frequency bands. For each FEKO run 4 frequency sweeps are taken in the passband frequency ranges. For this case, we set  $S_p = \{3.55, 3.6, 5.75, 5.8\}$ . The design parameters for the best filter design obtained by SaDE are shown in Table 1. Figure 3 shows the simulated frequency response of this design. The simulated current distribution for the 3.6 GHz and 5.8 GHz frequencies is presented in Figure 4, where the resonating ring in each case is clearly seen. In the first passband between 3.508 and 3.809 GHz, the filter has a return loss greater than 10 dB and insertion loss less than 0.5 dB. In the second passband between 5.744 and 6.121 GHz, the results also show a return loss greater than 10 dB and insertion loss less than 0.5 dB. The rejection band (between 4.236 and 5.367 GHz) has an insertion loss less than 20 dB. In the first passband, the return loss is greater than 29 dB at both 3.533 GHz and 3.759 GHz. In the second passband the return loss is greater than 22 dB at 5.794 GHz and greater than 28 dB at 6.07 GHz.

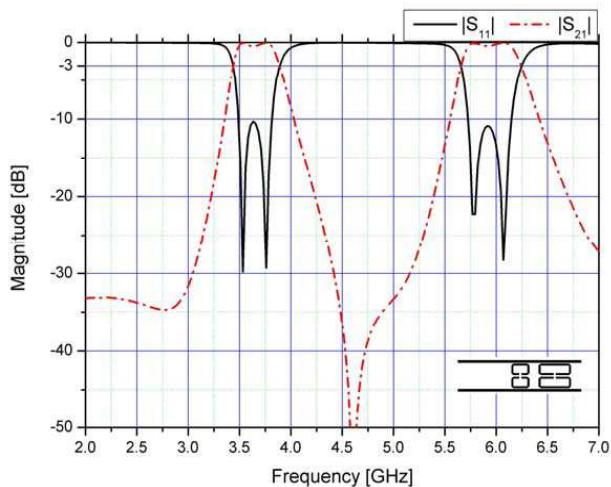


**Figure 3.** Simulated frequency response of the dual-band filter.

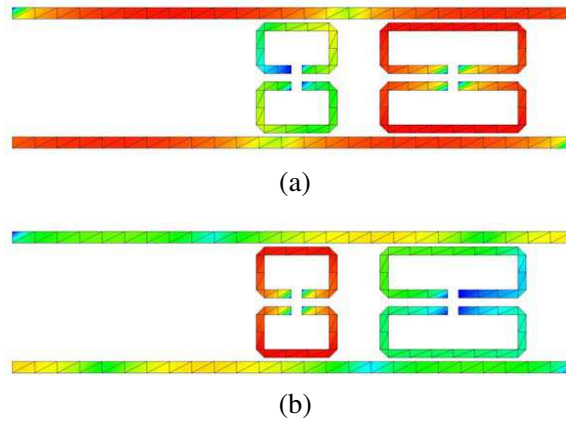


**Figure 4.** Current distribution simulations for dual-band filter at (a) 3.5 GHz and (b) 5.8 GHz.

**Table 1.** Design parameters for the dual-band filter design case (mm).

$W_1$	0.56	$L_1$	27.81
$W_2$	0.41	$L_2$	2.32
$S_1$	0.41	$L_3$	6.43
$S_2$	0.20	$L_4$	1.71
$S_3$	0.54	$L_5$	3.21
$G$	2.12		

#### 4.2. Tri-band Filter Design Case

The tri-band filter is designed for operation in two WiMax (IEEE 802.16) and one WiFi (IEEE 802.11b/g) frequency bands. These are the 2.4 GHz, 3.5 GHz, and the 5.8 GHz frequency bands. For each FEKO run, six frequency sweeps are taken in the passband frequency ranges. For this case, we set  $S_p = \{2.35, 2.4, 3.55, 3.6, 5.75, 5.8\}$ . The execution time for each algorithm run as it is expected increases compared with the dual-band case. The increase in time is about 60% more than time required for the dual-band case. The design parameters for the best filter design obtained by SaDE are shown in Table 2. Figure 5 shows the simulated frequency response of the tri-band filter design. The simulated current distribution for the 2.4 GHz, 3.6 GHz and 5.8 GHz frequencies is presented in Figure 6, where the resonating ring in each case is clearly seen. In the first passband between 2.377 and 2.553 GHz, the filter has a return loss greater than 10 dB and

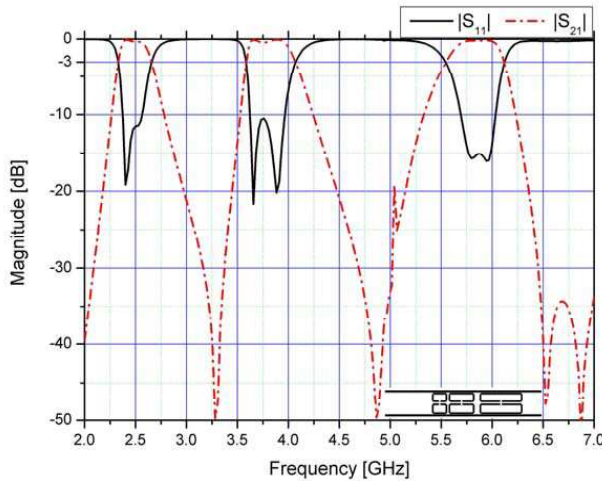


**Figure 5.** Simulated frequency response of the tri-band filter.

**Table 2.** Design parameters for the tri-band filter design case (mm).

$W_1$	0.50	$L_1$	40.00
$W_2$	0.41	$L_2$	4.85
$S_1$	0.40	$L_3$	10.15
$S_2$	0.11	$L_4$	1.87
$S_3$	0.39	$L_5$	3.10
$G_1$	1.30	$L_6$	5.80
$G_2$	0.35		

insertion loss less than 0.4 dB. The resonant frequency is at 2.402 GHz with return loss greater than 19 dB and insertion loss less than 0.08 dB. In the second passband between 3.633 and 3.96 GHz, the return loss is greater than 10 dB and the insertion loss is less than 0.5 dB. The return loss is greater than 22 dB at both 3.658 and 3.884 GHz. The first rejection band (between 2.980 and 3.432 GHz) has an insertion loss less than 20 dB. The third passband is between 5.693 and 6.020 GHz. The return loss is greater than 10 dB and the insertion loss less than 0.6 dB. The resonant frequency is at 5.945 GHz with return loss greater than 16 dB and insertion loss less than 0.2 dB. The second rejection band (between 4.487 and 5.141 GHz) has an insertion loss less than 20 dB.

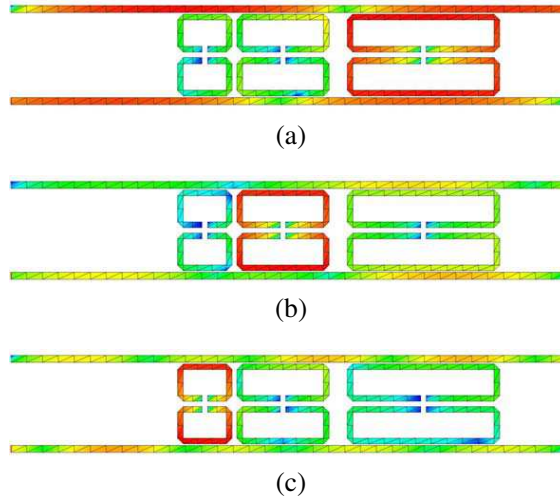


**Figure 6.** Current distribution simulations for tri-band filter at (a) 2.4 GHz, (b) 3.65 GHz, and (c) 5.8 GHz.

## 5. CONCLUSION

In this paper, we have presented a design methodology for microwave filters based on differential evolution. Two design cases of dual and tri-band operation for WiFi and WiMax applications have been presented. The filter best results found exhibit low loss in the passbands and high isolation between the passbands. The DE algorithms are robust optimizers. The proposed synthesis procedure can be used to any filter design problem that requires optimization of the geometry parameters. The correct selection of the objective function is essential for the efficient application of the SaDE algorithm. In classical DE algorithms, the selection of the appropriate strategy for trial vector generation and control parameters requires additional computational time using a trial-and-error search procedure. Therefore, it is not always an easy task to fine-tune the control parameters and strategy given also that commonly the appropriate control parameters and strategy selection are problem dependent. The SaDE advantage though, is the fact that no additional time for solving a given problem is required. SaDE requires only the adjustment of two parameters: the population size and the number of iterations. The filter design cases presented show the applicability of this design method. In our future work, we plan to explore the SaDE algorithm applicability to other design problems in electromagnetics.

## ACKNOWLEDGMENT

The authors would like to thank Professor P. N. Suganthan for proving the source code of the SaDE algorithm.

## REFERENCES

1. Wang, X. H., B. Z. Wang, and K. J. Chen, "Compact broadband dual-band bandpass filters using slotted ground structures," *Progress In Electromagnetics Research*, Vol. 82, 151–166, 2008.
2. Wang, Z., Q. Lai, R. Xu, B. Yan, W. Lin, and Y. Guo, "A millimeter-wave ultra-wideband four-way switch filter module based on novel three-line microstrip structure band-pass filters," *Progress In Electromagnetics Research*, Vol. 94, 297–309, 2009.
3. Siakavara, K. and C. Damianidis, "Microwave filtering in waveguides loaded with artificial single or double negative materials realized with dielectric spherical particles in resonance," *Progress In Electromagnetics Research*, Vol. 95, 103–120, 2009.
4. Razalli, M. S., A. Ismail, M. A. Mahdi, and M. N. Hamidon, "Novel compact 'via-less' ultra-wide band filter utilizing capacitive microstrip patch," *Progress In Electromagnetics Research*, Vol. 91, 213–227, 2009.
5. Mo, S. G., Z. Y. Yu, and L. Zhang, "Design of triple-mode bandpass filter using improved hexagonal loop resonator," *Progress In Electromagnetics Research*, Vol. 96, 117–125, 2009.
6. Liu, C. C., Y. H. Chang, T. J. Yang, and C. J. Wu, "Narrowband filter in a heterostructured multilayer containing ultrathin metallic films," *Progress In Electromagnetics Research*, Vol. 96, 329–346, 2009.
7. Zhang, L., Z. Yu, and S. Mo, "Novel planar multimode bandpass filters with radial-line stubs," *Progress In Electromagnetics Research*, Vol. 101, 33–42, 2010.
8. Ye, C. S., Y. K. Su, M. H. Weng, C. Y. Hung, and R. Y. Yang, "Design of the compact parallel-coupled lines wideband bandpass filters using image parameter method," *Progress In Electromagnetics Research*, Vol. 100, 153–173, 2010.
9. Oraizi, H. and M. S. Esfahlan, "Optimum design of lumped filters incorporating impedance matching by the method of least squares," *Progress In Electromagnetics Research*, Vol. 100, 83–103, 2010.
10. Dai, G. L. and M. Y. Xia, "Novel miniaturized bandpass filters

- using spiral-shaped resonators and window feed structures,” *Progress In Electromagnetics Research*, Vol. 100, 235–243, 2010.
11. Wang, Z. G., X. Q. Li, S. P. Zhou, B. Yan, R. M. Xu, and W. G. Lin, “Half mode substrate integrated folded waveguide (HMSIFW) and partial  $H$ -plane bandpass filter,” *Progress In Electromagnetics Research*, Vol. 101, 203–216, 2010.
  12. Yang, M. H., J. Xu, Q. Zhao, L. Peng, and G. P. Li, “Compact, broad-stopband lowpass filters using SIRs-loaded circular hairpin resonators,” *Progress In Electromagnetics Research*, Vol. 102, 95–106, 2010.
  13. Velazquez-Ahumada, M. D. C., J. Martel, F. Medina, and F. Mesa, “Application of stub loaded folded stepped impedance resonators to dual band filter design,” *Progress In Electromagnetics Research*, Vol. 102, 107–124, 2010.
  14. Vegesna, S. and M. Saed, “Novel compact dual-band bandpass microstrip filter,” *Progress In Electromagnetics Research B*, Vol. 20, 245–262, 2010.
  15. Chen, C. Y. and C. Y. Hsu, “A simple and effective method for microstrip dual-band filters design,” *IEEE Microwave and Wireless Components Letters*, Vol. 16, 246–248, 2006.
  16. Zhang, X. Y., J. X. Chen, Q. Xue, and S. M. Li, “Dual-band bandpass filters using stub-loaded resonators,” *IEEE Microwave and Wireless Components Letters*, Vol. 17, 583–585, 2007.
  17. Mondal, P. and M. K. Mandal, “Design of dual-band bandpass filters using stub-loaded open-loop resonators,” *IEEE Transactions on Microwave Theory and Techniques*, Vol. 56, 150–155, 2008.
  18. Lai, X., B. Wu, T. Su, and C. H. Liang, “A novel tri-band filter using stub-loaded open loop ring resonators,” *Microwave and Optical Technology Letters*, Vol. 52, 523–526, 2010.
  19. Koziel, S. and J. W. Bandler, “Space mapping with multiple coarse models for optimization of microwave components,” *IEEE Microwave and Wireless Components Letters*, Vol. 18, 1–3, 2008.
  20. FEKO, “User’s Manual, FEKO Suite 5.2,” [www.feko.info](http://www.feko.info), 2003.
  21. Goudos, S. K., Z. D. Zaharis, M. Salazar-Lechuga, P. I. Lazaridis, and P. B. Gallion, “Dielectric filter optimal design suitable for microwave communications by using multiobjective evolutionary algorithms,” *Microwave and Optical Technology Letters*, Vol. 49, 2324–2329, 2007.
  22. Mallahzadeh, A. R., H. Oraizi, and Z. Davoodi-Rad, “Application of the invasive weed optimization technique for antenna configurations,” *Progress In Electromagnetics Research*, Vol. 79,

- 137–150, 2008.
23. Lu, Z. B., A. Zhang, and X. Y. Hou, “Pattern synthesis of cylindrical conformal array by the modified particle swarm optimization algorithm,” *Progress In Electromagnetics Research*, Vol. 79, 415–426, 2008.
  24. Li, W. T., X. W. Shi, and Y. Q. Hei, “An improved particle swarm optimization algorithm for pattern synthesis of phased arrays,” *Progress In Electromagnetics Research*, Vol. 82, 319–332, 2008.
  25. Guney, K. and S. Basbug, “Interference suppression of linear antenna arrays by amplitude-only control using a bacterial foraging algorithm,” *Progress In Electromagnetics Research*, Vol. 79, 475–497, 2008.
  26. Panduro, M. A., C. A. Brizuela, L. I. Balderas, and D. A. Acosta, “A comparison of genetic algorithms, particle swarm optimization and the differential evolution method for the design of scannable circular antenna arrays,” *Progress In Electromagnetics Research B*, Vol.13, 171–186, 2009.
  27. Mallahzadeh, A. R., S. Es’haghi, and H. R. Hassani, “Compact U-array MIMO antenna designs using iwo algorithm,” *International Journal of RF and Microwave Computer-aided Engineering*, Vol. 19, 568–576, 2009.
  28. Mallahzadeh, A. R., S. Es’haghi, and A. Alipour, “Design of an E-shaped MIMO antenna using IWO algorithm for wireless application at 5.8 GHz,” *Progress In Electromagnetics Research*, Vol. 90, 187–203, 2009.
  29. Lanza, M., J. R. Perez Lopez, and J. Basterrechea, “Synthesis of planar arrays using a modified particle swarm optimization algorithm by introducing a selection operator and elitism,” *Progress In Electromagnetics Research*, Vol. 93, 145–160, 2009.
  30. Khodier, M. M. and M. Al-Aqeel, “Linear and circular array optimization: A study using particle swarm intelligence,” *Progress In Electromagnetics Research B*, Vol. 15, 347–373, 2009.
  31. Siakavara, K., “Novel fractal antenna arrays for satellite networks: Circular ring sierpinski carpet arrays optimized by genetic algorithms,” *Progress In Electromagnetics Research*, Vol. 103, 115–138, 2010.
  32. Goudos, S. K. and J. N. Sahalos, “Pareto optimal microwave filter design using multiobjective differential evolution,” *IEEE Transactions on Antennas and Propagation*, Vol. 58, 132–144, 2010.
  33. Dib, N. I., S. K. Goudos, and H. Muhsen, “Application

- of Taguchi's optimization method and self-adaptive differential evolution to the synthesis of linear antenna arrays," *Progress In Electromagnetics Research*, Vol. 102, 159–180, 2010.
34. Pal, S., S. Das, A. Basak, and P. N. Suganthan, "Synthesis of difference patterns for monopulse antennas with optimal combination of array-size and number of subarrays — A multi-objective optimization approach," *Progress In Electromagnetics Research B*, Vol. 21, 257–280, 2010.
  35. Pal, S., B. Qu, S. Das, and P. N. Suganthan, "Linear antenna array synthesis with constrained multi-objective differential evolution," *Progress In Electromagnetics Research B*, Vol. 21, 87–111, 2010.
  36. Carro, P. L., J. de Mingo, and P. G. Ducar, "Radiation pattern synthesis for maximum mean effective gain with spherical wave expansions and particle swarm techniques," *Progress In Electromagnetics Research*, Vol. 103, 355–370, 2010.
  37. Karimkashi, S. and A. A. Kishk, "Invasive weed optimization and its features in electromagnetics," *IEEE Transactions on Antennas and Propagation*, Vol. 58, 1269–1278, 2010.
  38. Chamaani, S., M. S. Abrishamian, and S. A. Mirtaheri, "Time-domain design of UWB vivaldi antenna array using multiobjective particle swarm optimization," *IEEE Antennas and Wireless Propagation Letters*, Vol. 9, 666–669, 2010.
  39. Storn, R. and K. Price, "Differential evolution — A simple and efficient adaptive scheme for global optimization over continuous spaces," Tech. Rep. TR-95-01, <http://citeseer.ist.psu.edu/article/storn95differential.html>, 1995.
  40. Storn, R. and K. Price, "Differential evolution — A simple and efficient heuristic for global optimization over continuous spaces," *Journal of Global Optimization*, Vol. 11, 341–359, 1997.
  41. Cheong, F. and R. Lai, "Designing a hierarchical fuzzy logic controller using the differential evolution approach," *Applied Soft Computing*, Vol. 7, 481–491, 2007.
  42. Kukkonen, S., S. R. Jangam, and N. Chakraborti, "Solving the molecular sequence alignment problem with generalized differential evolution 3 (GDE3)," *Proceedings of IEEE Symposium on Computational Intelligence in Multicriteria Decision Making*, 302–309, 2007.
  43. Das, S. and A. Konar, "Automatic image pixel clustering with an improved differential evolution," *Applied Soft Computing*, Vol. 9, 226–236, 2009.
  44. Brest, J., S. Greiner, B. Boskovic, M. Mernik, and V. Zumer,

- “Self-adapting control parameters in differential evolution: A comparative study on numerical benchmark problems,” *IEEE Transactions on Evolutionary Computation*, Vol. 10, 646–657, 2006.
45. Goudos, S. K., “Design of microwave broadband absorbers using a self-adaptive differential evolution algorithm,” *International Journal of RF and Microwave Computer-aided Engineering*, Vol. 19, 364–372, 2009.
  46. Qin, A. K. and P. N. Suganthan, “Self-adaptive differential evolution algorithm for numerical optimization,” *The 2005 IEEE Congress on Evolutionary Computation*, Vol. 2, 1785–1791, 2005.
  47. Huang, V. L., A. K. Qin, and P. N. Suganthan, “Self-adaptive differential evolution algorithm for constrained real-parameter optimization,” *The 2006 IEEE Congress on Evolutionary Computation*, 215–222, 2006.
  48. Qin, A. K., V. L. Huang, and P. N. Suganthan, “Differential evolution algorithm with strategy adaptation for global numerical optimization,” *IEEE Transactions on Evolutionary Computation*, Vol. 13, 398–417, 2009.
  49. Storn, R., “Differential evolution research — Trends and open questions,” *Studies in Computational Intelligence*, Vol. 143, 1–31, 2008.
  50. Mezura-Montes, E., J. Velazquez-Reyes, and C. A. Coello Coello, “A comparative study of differential evolution variants for global optimization,” *ECCO 2006 — Genetic and Evolutionary Computation Conference*, 485–492, Seattle, WA, 2006.
  51. Iorio, A. W. and X. Li, “Solving rotated multi-objective optimization problems using differential evolution,” *Lecture Notes in Artificial Intelligence (Subseries of Lecture Notes in Computer Science)*, Vol. 3339, 861–872, 2004.